Theoret. Appl. Mech., Vol.31, No.2, pp.153–188, Belgrade 2004

Hydrodynamic forces on two moving discs

D. A. Burton * **J. Gratus** † **R. W. Tucker** ‡

Abstract

We give a detailed presentation of a flexible method for constructing explicit expressions of irrotational and incompressible fluid flows around two rigid circular moving discs. We also discuss how such expressions can be used to compute the fluid-induced forces and torques on the discs in terms of Killing drives. Conformal mapping techniques are used to identify a meromorphic function on an annular region in $\mathbb{C}$ with a flow around two circular discs by a Möbius transformation. First order poles in the annular region correspond to vortices outside of the two discs. Inflows are incorporated by putting a second order pole at the point in the annulus that corresponds to infinity.

Keywords: *Killing drives, conformal mapping techniques, meromorphic function, Möbius transformation, annular region*

*Physics Department, Lancaster University, Lancaster, LA1 4YB, UK, e-mail: d.burton@lancaster.ac.uk

†Physics Department, Lancaster University, Lancaster, LA1 4YB, UK, e-mail: j@gratus.net

‡Physics Department, Lancaster University, Lancaster, LA1 4YB, UK, e-mail: robin.tucker@lancaster.ac.uk

1 Introduction

The ability to model the hydrodynamical interaction between rigid bodies immersed in a fluid is important in many engineering and physics problems. The most direct method of attack is to solve the coupled Navier-Stokes and rigid body system of equations for the instantaneous configurations of the fluid and bodies. This is, in general, a highly non-trivial exercise and often impossible without recourse to intensive computational fluid dynamics. If the characteristic Reynolds number associated with the fluid and body system is sufficiently high then, depending on the physical scenario, it may be reasonable to neglect fluid viscosity and adopt potential theory. Engineering problems that involve interacting rigid objects whose separation wakes can be neglected [20] and, for example, the astrophysical interaction of magnetic flux tubes in stars [5] are all amenable to potential theory. If vorticity is an important ingredient in the physical picture, e.g. consider a set of interacting marine risers undergoing vortex-induced vibration in the subcritical Reynolds number range, then *irrotational* (instead of *potential*) flows are more applicable. In such situations there is no single-valued velocity potential on the entire flow region. Irrotational flow theory is the basis of *discrete vortex models* (see, for example, [16, 7] and [15] for a review) of vortex-induced vibration of a circular disc in unbounded 2-dimensional flow. In such methods the wake behind the disc is represented by a dynamical set of point singularities (so-called *point vortices* [2, 12]) in the fluid velocity. The instantaneous flow velocity field is determined by the position and strength of each vortex and the position and velocity of the circular disc using Milne-Thomson's circle theorem [12]. The fluid velocity is used to calculate the fluid pressure and leads to the fluid-induced force on the disc. The vorticies are convected with the flow, and so are influenced by the positions and strengths of the other vorticies and the position and velocity of the disc. The crucial consequences of non-zero viscosity, i.e. the generation and dissipation of vorticity, are put into the model using boundary-layer methods [17, 21] and heuristics [16, 7]. Although such models are quite crude in comparison with detailed numerical simulations involving the Navier-Stokes equations their predictions are acceptable [16, 14, 7] if the heuristics are carefully tuned.

The model discussed in [16, 7] can be generalized to discs of non-circular cross-section using conformal mapping techniques. The non-circularity of the disc means that a non-trivial fluid torque, as well as a force, will be applied to it. An application to the coupled motion of a cable and an adhered rain rivulet induced by light wind and rain conditions on a cable-stayed bridge is given in [6]. To apply the discrete vortex method to the vortex-induced vibration of more than one object in an unbounded region, e.g. a *set* of interacting marine risers, is a more complicated venture. As a prototype model of this problem we consider in this article arbitrary irrotational flows outside two circular moving discs. In principle the method can be adapted to accommodate discs with more general cross-sections by using a different conformal map from the Möbius map used here.

The earliest discussions of potential flows around two discs are due to Hicks [10], Greenhill [8] and Bassett [3]. Hicks' motivation was to analyse the motion of a cylindrical pendulum inside another cylinder filled with fluid. Yamamoto [20] used Milne-Thomson's circle theorem in an iterative scheme that yields potential flow due to an inflow around *any* number of discs but did not discuss the effects of point vorticies. Probably the most common method of analysing potential flow around two discs is via bipolar coordinates [13] as used in, for example, [3, 5, 9]. Once the fluid velocity has been constructed the force and torque on a body is obtained by pressure integrals [2, 11, 7] and an appeal to the Euler equations. An alternative method of obtaining the force and torque, where again an explicit expression for the fluid velocity is required, is Thomson and Tait's variational approach [11] used in, for example, [5, 18]. This method relies on the fluid kinetic energy being bounded, which is not true if the flow contains point vorticies.

Our proposed method for the calculation of arbitrary irrotational flows around two circular discs is more flexible than those given before. The approach is to construct the complex velocity due to an inflow and a set of point vortices using doubly-periodic (elliptic) functions represented in terms of the first Jacobi theta function θ_1 and its derivatives. The power of the method is in the freedom to choose the representation of θ_1 and thus optimize the calculation for either numerical or analytical purposes. We begin by constructing flows around two stationary discs and then generalize the results to the moving scenario.

2 Background

Many tensors and maps in this article are to be regarded implicitly as one-parameter families with universal time t as the parameter. The coordinate components, with respect to any chart, of such objects are smooth with respect to t. We denote the partial t-derivative of such a tensor T by $\partial_t T$. For example, if α is a such a differential 1-form

$$\alpha = \alpha_a(x;t)dx^a, \tag{1}$$

$$\partial_t \alpha \equiv \frac{\partial \alpha_a}{\partial t}(x;t)dx^a \tag{2}$$

with respect to a chart $\{x^a\}$. The semicolon is a reminder that t has a special status and is *not* to be regarded as a coordinate. Let c be a t-dependent p-chain on a differential manifold $\mathcal{M}$,

$$\begin{aligned} c : [0,1]^p &\to \mathcal{M} \\ (\xi;t) &\to x^a = c^a(\xi;t), \end{aligned} \tag{3}$$

where $\xi \equiv (\xi^1, \xi^2, \ldots, \xi^p)$. The *velocity* of c, denoted by $\dot{c}$, is the vector field (attached to c)

$$\dot{c} \equiv \frac{\partial c_a}{\partial t}(\xi; t)\frac{\partial}{\partial x^a}. \tag{4}$$

If a differential manifold $\mathcal{M}$ possesses a metric $g \in \mathbf{T}^0_2\mathcal{M}$ then the *metric dual* $\tilde{X}$ of a vector field $X \in \Gamma T\mathcal{M}$ is the differential 1-form $\tilde{X} \equiv g(X, -) \in \Gamma T^*\mathcal{M}$. Similarly, the metric dual $\tilde{\alpha} \in \Gamma T\mathcal{M}$ of a differential 1-form $\alpha \in \Gamma T^*\mathcal{M}$ is the vector field $Y \in \Gamma T\mathcal{M}$ such that $\tilde{Y} = \alpha$. Note that $\tilde{\tilde{Y}} = Y$. The symbol $\mathcal{F}(\mathcal{M})$ denotes the space of scalar functions on $\mathcal{M}$ and $\Lambda_p\mathcal{M}$ denotes the bundle of differential p-forms on $\mathcal{M}$. The Lie derivative of the tensor $T \in \Gamma\mathbf{T}^p_q\mathcal{M}$ with respect to the vector field X is denoted by $\mathcal{L}_X T$.

2.1 Killing drive on a lamina

Let $\mathcal{M}$ be a 2-dimensional flat Riemannian manifold with metric g, Hodge map $\star$ and Levi-Civita connection ∇. Let $V \in \Gamma T\mathcal{M}$ be the Eulerian velocity vector field of an inviscid, incompressible and irrotational Newtonian fluid flow on $\mathcal{M}$. Thus V is a solution of the Euler equations

$$\partial_t\tilde{V} + \nabla_V\tilde{V} = -dp, \tag{5}$$

$$d \star \tilde{V} = 0, \tag{6}$$

where $p \in \mathcal{F}(\mathcal{M})$ is the fluid *pressure* and

$$d\tilde{V} = 0. \tag{7}$$

The topology of $\mathcal{M}$ is non-trivial in order to accommodate the presence of rigid bodies and point vorticies (point singularities in the fluid flow). We require that the topology of $\mathcal{M}$ is such that there exists a *global* chart $\{x, y\}$ on $\mathcal{M}$ with respect to which the metric has the form

$$g = dx \otimes dx + dy \otimes dy. \tag{8}$$

Such a chart will be called *cartesian*.

The Poincaré lemma [1] allows us to solve (7) on some open set $\mathcal{N} \subset \mathcal{M}$ in terms of a *velocity potential* $\varphi \in \mathcal{F}(\mathcal{N})$,

$$\tilde{V} = d\varphi. \tag{9}$$

The *circulation* $\Gamma_V[\gamma]$ of V around a closed curve γ on $\mathcal{M}$ is

$$\Gamma_V[\gamma] \equiv \int_\gamma \tilde{V}. \tag{10}$$

If there exists a potential for V on *all* of $\mathcal{M}$, i.e. $\Gamma_V[\gamma] = 0$ for all γ, then the fluid flow is called *potential*. 2-dimensional fluid flows with immersed rigid bodies may, and with point vorticies certainly, possess circulation. For such V there exists a closed curve γ such that $\Gamma_V[\gamma] \neq 0$.

Let $C : \lambda \in [0,1] \to \mathcal{M}$ be a closed 1-chain representing the boundary of a compact body (a *lamina*) in $\mathbb{R}^2$ at time t. Let $\dot{C}$ be the velocity of C, i.e. the vector field

$$\dot{C} \equiv \partial_t C^a(\lambda; t) \frac{\partial}{\partial x^a} \tag{11}$$

attached to C on $\mathcal{M}$. The functions $x^a = C^a(\lambda; t)$ are the components of C (at time t) with respect to a chart on $\mathcal{M}$ with coordinates $\{x^a\}$. The *Eulerian velocity* of C is a vector field $U_C \in \Gamma T\mathcal{M}$ such that

$$U_C \big|_C = \dot{C}. \tag{12}$$

The choice of U_C is clearly non-unique. However, it can be shown that for any solution to (12)

$$\partial_t(C^*\alpha) = C^*\big(\partial_t\alpha + \mathcal{L}_{U_C}\alpha\big) \tag{13}$$

for any differential form α on $\mathcal{M}$. If the lamina boundary C is *rigid* then

$$C^*\big(\mathcal{L}_{U_C} g\big) = 0. \tag{14}$$

Equations (6) and (7) are solved subject to the *no-through-flow* boundary condition on C,

$$g(V, N_C) = g(U_C, N_C), \tag{15}$$

where N_C is normal to C or, equivalently,

$$C^* \star (\tilde{V} - \tilde{U}_C) = 0. \tag{16}$$

The fluid pressure p is used to construct the *Killing drive* $F_K[C]$ of K on C,

$$F_K[C] = -\int_C p \star \tilde{K}, \tag{17}$$

where K is a Killing vector of g

$$\mathcal{L}_K g = 0. \tag{18}$$

Equation (17) is a unified expression for the fluid force and torque on C (see [7] for further discussion). The topology of $\mathcal{M}$ is such that *globally*

$$\star\tilde{K} = d\zeta_K \tag{19}$$

where the scalar $\zeta_K \in \mathcal{F}(\mathcal{M})$ is called a *Killing potential* of K. This follows by noting that with respect to a cartesian chart $\{x, y\}$ (see equation (8)) any K on $\mathcal{M}$ can be written

$$K = a\frac{\partial}{\partial x} + b\frac{\partial}{\partial y} + c\left(x\frac{\partial}{\partial y} - y\frac{\partial}{\partial x}\right), \tag{20}$$

$$da = db = dc = 0 \tag{21}$$

where $a, b, c \in \mathcal{F}(\mathcal{M})$ are t-dependent constants. Any associated potential ζ_K is then of the form

$$\zeta_K = ay - bx - c\frac{1}{2}(x^2 + y^2) + f, \tag{22}$$

$$df = 0 \tag{23}$$

where $f \in \mathcal{F}(\mathcal{M})$ is a t-dependent constant. Therefore, equation (17) can be written

$$F_K[C] = \int_C \zeta_K dp \tag{24}$$

since $\partial C = 0$. Using (5), (6), (7), (13), (16), $\partial C = 0$ and

$$\mathcal{L}_V \tilde{V} = \nabla_V \tilde{V} + \frac{1}{2} d[g(V, V)], \tag{25}$$

to manipulate (24) one obtains

$$F_K[C] = -\frac{d}{dt}\int_C \zeta_K \tilde{V} + \int_C \partial_t \zeta_K \tilde{V} + \int_C \left(\frac{1}{2} g(V, V) \star \tilde{K} - g(V, K) \star \tilde{V}\right) \tag{26}$$

in terms of the Killing potential ζ_K and V. Once V has been determined and ζ_K chosen the Killing drive $F_K[C]$ on each C can be calculated using (26). An example is given in reference [7] where the force on an isolated circular disc due to a set of point vortices is discussed. Useful Killing potentials adapted to C are shown in table 1.

2.2 Complexification of $\mathbb{R}^2$

As before, let $\{x, y\}$ be the components of a cartesian chart on $\mathcal{M}$, i.e.

$$g = dx \otimes dx + dy \otimes dy. \tag{27}$$

Table 1: Useful Killing potentials adapted to C and their associated Killing drives on C. The point $(x_0, y_0) \in \mathbb{R}^2$ is fixed in the lamina bounded by C and is t-dependent.

Killing potential ζ_K	Killing drive $F_K[C]$
$-y + y_0$	x-component of fluid force on C
$x - x_0$	y-component of fluid force on C
$-[(x - x_0)^2 + (y - y_0)^2]/2$	fluid torque about (x_0, y_0) on C

globally, and introduce the complexification of $\mathbb{R}^2$ given by $z = x + iy$. The complex conjugate of an *expression* f containing z is denoted $\bar{f}$. We define the complex conjugate $f^\dagger$ of a *function* $f : \mathbb{C} \to \mathbb{C}$ to be

$$f^\dagger(z) \equiv \overline{f(\bar{z})} \tag{28}$$

The Hodge map $\star$ is a linear automorphism on the vector space of 1-forms on 2-dimensional manifolds. The operator P

$$P \equiv \frac{1}{2}(1 - i\star) \tag{29}$$

satisfies $P^2 = P$ on sections of $\Lambda_1\mathcal{M}$. It follows that

$$Pdz = dz, \tag{30}$$

$$Pd\bar{z} = 0. \tag{31}$$

For simplicity, we will use the same symbol for real manifolds and their complexifications.

2.3 Fluid velocities and potentials

Using equations (6), (7) and (29) we see that

$$dP\tilde{V} = 0 \tag{32}$$

and since

$$\tilde{V} = \frac{1}{2}\big(\bar{v}dz + vd\bar{z}\big) \tag{33}$$

where

$$v \equiv dz(V) \tag{34}$$

it follows from (32) that

$$d\nu = 0 \tag{35}$$

where $\nu = \bar{v}dz$ is called the *complex velocity* 1*-form*.

Equation (35) indicates that the component $\bar{v}$ (called the *complex velocity*) of ν with respect to z does not contain $\bar{z}$.

Using the Poincaré lemma [1] to solve (35) we obtain the local expression

$$\nu = dW \tag{36}$$

on some open subset $\mathcal{N}$ of $\mathcal{M}$. The scalar $W \in \mathcal{F}(\mathcal{N})$ is a holomorphic function known as a *complex potential* (for ν). The velocity vector field V is

$$V = \widetilde{\Re(\nu)}. \tag{37}$$

2.4 No-through-flow boundary condition on a stationary boundary

Let C be a closed curve on $\mathcal{M}$ that represents a physical solid boundary. The no-through-flow boundary condition on V for a *stationary* C is

$$C^* \star \tilde{V} = 0 \tag{38}$$

which can also be written

$$\Im\big(C^* P\tilde{V}\big) = 0 \tag{39}$$

or

$$\begin{aligned}\Im\big(C^*\nu\big) &= \Im\big(C^* dW\big)\\ &= d[C^*\Im(W)]\\ &= 0.\end{aligned} \tag{40}$$

Thus, another way of expressing the no-through-flow condition on a stationary boundary is that $\Im(W)$ is constant on the image of C.

2.5 Construction of flows by conformal techniques

Let $W_{\mathcal{V}} \in \mathcal{F}(\mathcal{V})$, $\mathcal{V} \subset \mathbb{C}$ be a complex potential that satisfies the no-through-flow boundary condition on a stationary $\mathcal{B} \subset \mathcal{V}$. Then, given a diffeomorphism (a conformal map) $\varphi : \mathcal{U} \subset \mathbb{C} \to \mathcal{V}$ one obtains a complex potential $W_{\mathcal{U}} = \varphi^* W_{\mathcal{V}}$ on $\mathcal{U}$ that satisfies the no-through-flow boundary condition on $\varphi^{-1}(\mathcal{B})$. For a traditional introduction to the application of conformal techniques to fluid dynamics see [12].

2.6 Elliptic functions

A holomorphic function f that satisfies

$$f(z + 2\omega_1) = f(z), \tag{41}$$

$$f(z + 2\omega_2) = f(z) \tag{42}$$

where $\omega_1, \omega_2 \in \mathbb{C}$, $\omega_1/\omega_2 \notin \mathbb{R}$, for each z at which $f(z)$ exists is called *doubly-periodic* [19]. A doubly-periodic function that is analytic except at isolated singularities is said to be *elliptic* [19]. A *cell* of an elliptic function f is a parallelogram $\mathcal{C}_z = \{z + 2\omega_1\lambda + 2\omega_2\mu; 0 \leq \lambda <$

$1, 0 \leq \mu < 1\}$ in $\mathbb{C}$ where z is chosen such that no poles of f lie on the boundary of $\mathcal{C}_z$. From the Liouville theorem [19], any elliptic function is completely specified (up to a constant) by the locations and coefficients of its poles within any cell. Let f have n poles located at $\{\beta_1, \ldots, \beta_n\}$ with orders $\{m_1, \ldots, m_n\}$ respectively. If the principle part f_r of f at β_r, $r \in \{1, \ldots, n\}$, is

$$f_r(z) = \sum_{m=1}^{m_r} A_{r,m}(z - \beta_r)^{-m} \tag{43}$$

and $\Im(\omega_2/\omega_1) > 0$ then f can be represented[1]

$$f(z) = A_0 + \sum_{r=1}^{n} \sum_{m=1}^{m_r} \frac{(-1)^{m-1} A_{r,m}}{(m-1)!} \frac{d^m}{dz^m} \log \theta_1\left(\frac{\pi z - \pi\beta_r}{2\omega_1} \,\middle|\, \frac{\omega_2}{\omega_1} \right) \tag{44}$$

where $\theta_1(z|\tau) \equiv \theta_1(z, e^{i\pi\tau})$,

$$\theta_1(z, q) \equiv 2 \sum_{n=0}^{\infty} (-1)^n q^{(n+1)^2} \sin\big[(2n+1)z\big] \quad \text{with } |q| < 1, \tag{45}$$

is the first Jacobi theta function. Its properties are discussed comprehensively in chapter 21 of [19]. It can be shown that the residues of any elliptic function within the boundary of any cell must sum to zero [19]. Thus, the coefficients $\{A_{r,1}\}$ cannot be chosen arbitrarily and must satisfy

$$\sum_{r=1}^{n} A_{r,1} = 0. \tag{46}$$

[1] Theta functions are not the only way to represent elliptic functions. See reference [19] for other choices.

3 Irrotational fluid flow on an annulus

3.1 Doubly-periodic flows

Let $f : \mathbb{C} \to \mathbb{C}$ be an elliptic function where

$$f(z + 2\pi i) = f(z), \tag{47}$$
$$f(z - 2\omega) = f(z) \tag{48}$$

and $\omega \in \mathbb{R}$, $\omega > 0$ i.e. choose $\omega_1 = 2\pi i$ and $\omega_2 = -\omega$ in (41) and (42). The choice of sign of ω_2 ensures that $\Im(\omega_2/\omega_1) > 0$. Let $v : \mathbb{C} \to \mathbb{C}$ be the complex velocity on $\mathbb{C}$ given by

$$\bar{v} = v^\dagger(z) = f(z) - f^\dagger(-z). \tag{49}$$

Theorem 1. *The function $v^\dagger$ satisfies the no-through-flow condition on $\{n\omega + iy; n \in \mathbb{Z}, y \in \mathbb{R}\}$.*

Proof. We express the no-through-flow condition as $\Re[v^\dagger(z_0)] = 0$ $\forall$ $z_0 \in \{n\omega + iy; n \in \mathbb{Z}, y \in \mathbb{R}\}$. The cases of even and odd n are handled separately.
Even n :

$$\begin{aligned} v^\dagger(iy) &= f(iy) - f^\dagger(-iy) \\ &= 2i\Im[f(iy)], \end{aligned} \tag{50}$$

using (49), and hence $\Re[v^\dagger(iy)] = 0$. Appealing to (48) we find that $\Re[v^\dagger(n\omega + iy)] = 0$.
Odd n :

$$\begin{aligned} v^\dagger(\omega + iy) &= f(\omega + iy) - f^\dagger(-\omega - iy) \\ &= f(\omega + iy) - f^\dagger(\omega - iy) \\ &= 2i\Im[f(\omega + iy)], \end{aligned} \tag{51}$$

using (49) and (48).Thus $\Re[v^\dagger(\omega + iy)] = 0$ and appealing to (48) we conclude that $\Re[v^\dagger(n\omega + iy)] = 0$. □

A complex potential $W_{\mathcal{C}}$ for $v^\dagger_{\mathcal{C}}$ ($v^\dagger$ restricted to the cell $\mathcal{C} \equiv \mathcal{C}_0 = \{-2\omega\lambda + 2\pi\mu; 0 \le \lambda < 1, 0 \le \mu < 1\}$) is

$$W_{\mathcal{C}}(z) = F(z) + F^\dagger(-z) \tag{52}$$

where the first derivative of F,

$$F(z) = A_0 z + \sum_{r=1}^{n} \sum_{m=0}^{m_r - 1} \frac{(-1)^m A_{r,m+1}}{m!} \frac{d^m}{dz^m} \log \theta_1 \left(\frac{z - \beta_r}{2i} \,\middle|\, \frac{i\omega}{2\pi} \right), \tag{53}$$

with respect to z is the elliptic function f in (44) with $\omega_1 = 2\pi i$ and $\omega_2 = -\omega$.

3.2 Construction of flows on an annulus

Let exp be the exponential map

$$\begin{aligned} \exp : \mathcal{C} &\to \mathcal{A} \subset \mathbb{C} \\ z &\to \hat{z} = e^z \end{aligned} \tag{54}$$

restricted to the cell $\mathcal{C}$. Half of the image of exp is the annulus $\mathcal{A} \equiv \{re^{i\theta}; e^{-\omega} \le r < 1, 0 \le \theta < 2\pi i\}$ (see figure 1). Using $W_{\mathcal{C}}$ one can form the complex potential $W_{\mathcal{A}} = \log^* W_{\mathcal{C}}$ on $\mathcal{A}$ where log is the inverse of exp.

4 Irrotational fluid flow around two discs

4.1 Möbius transformation

Let $\mathcal{D}_1$ be the open unit disc in $\mathbb{C}$ centred at $0 \in \mathbb{C}$. Let $\mathcal{D}_2$ be another open disc in $\mathbb{C}$ where $\mathcal{D}_1 \cap \mathcal{D}_2 = \varnothing$. Let $\mathcal{E}$ denote the region outside of the discs, i.e. $\mathcal{E} \equiv \mathbb{C} \setminus (\mathcal{D}_1 \cup \mathcal{D}_2)$.

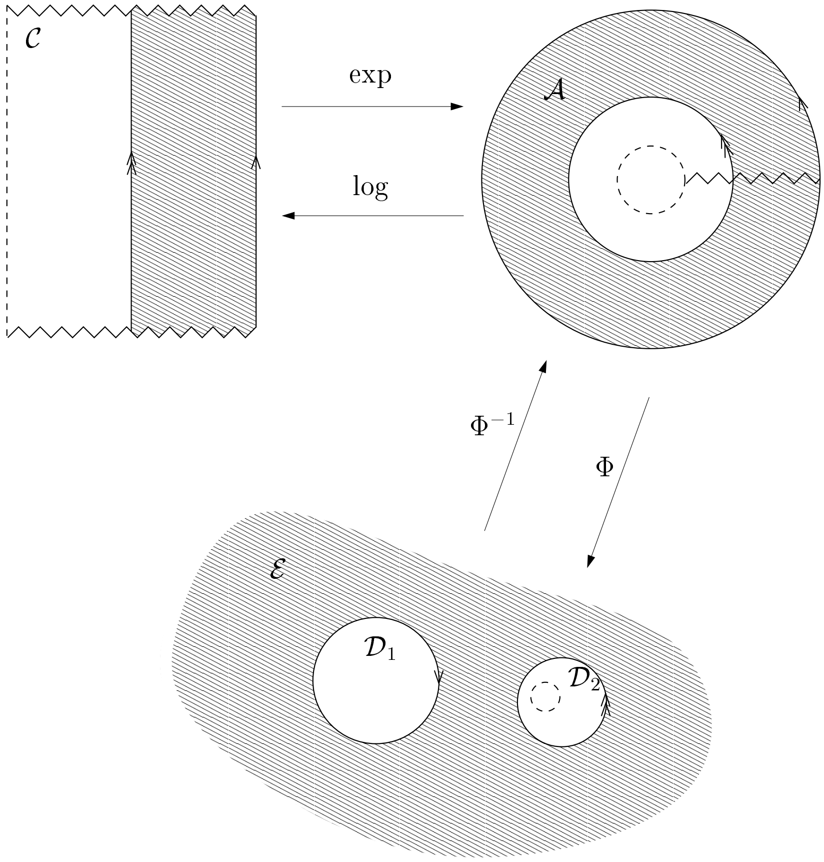

Figure 1: The annulus $\mathcal{A}$ is the exponential of half of the cell $\mathcal{C}$ (the shaded region), which itself is mapped by Φ into the region $\mathcal{E}$ outside of two open discs $\mathcal{D}_1$ and $\mathcal{D}_2$. The jagged lines at the top and bottom of $\mathcal{C}$ are identified to give the jagged line in $\mathcal{A}$. The arrows show how the boundary $b\mathcal{A}$ of $\mathcal{A}$, the boundary $b\mathcal{E}$ of $\mathcal{E}$ and the other two edges of $\mathcal{C}$ are identified. The left-hand (dotted) edge of $\mathcal{C}$ is mapped to a circle inside the inner edge of $\mathcal{A}$ and then to a circle in $\mathcal{D}_2$.

Theorem 2. *The Möbius map* Φ

$$\begin{aligned} \Phi : \mathcal{A} &\to \mathcal{E} \\ z \to \hat{z} &= \frac{z_\infty z - 1}{z - z_\infty} \end{aligned} \tag{55}$$

where $z_\infty \in \mathcal{A}$, $\Re(z_\infty) > 0$, $\Im(z_\infty) = 0$, *takes the outer edge of* $\mathcal{A}$ *(a unit disc) to the boundary of* $\mathcal{D}_1$. *The orientation of a closed curve* C *on the outer edge of* $\mathcal{A}$ *is opposite to that of* $\Phi \circ C$.

Proof. The unit disc in $\mathcal{A}$ is mapped to the unit disc in $\mathcal{E}$:
Introduce $c = 1/z_\infty$. Since

$$\begin{aligned} |\Phi(z)|^2 &= \frac{z - c}{cz - 1}\frac{\bar{z} - c}{c\bar{z} - 1} \\ &= \frac{z\bar{z} - c(z + \bar{z}) + c^2}{c^2 z\bar{z} - c(z + \bar{z}) + 1} \end{aligned} \tag{56}$$

we see that $|\Phi\big(e^{i\theta}\big)|$=1 where $\theta \in \mathbb{R}$.

The outer edge of $\mathcal{A}$ and the boundary of $\mathcal{D}_1$ have opposite orientations :

Their relative orientations are opposite if

$$\frac{1}{i}\frac{d}{d\theta}\log\Phi\big(e^{i\theta}\big) < 0. \tag{57}$$

The first derivative of Φ is

$$\Phi'(z) = \frac{c^2 - 1}{(cz - 1)^2} \tag{58}$$

and so

$$\frac{\Phi'(z)}{\Phi(z)} = \frac{c^2 - 1}{cz - 1}\frac{1}{z - c} \tag{59}$$

from which it follows

$$\begin{aligned}\frac{1}{i}\frac{d}{d\theta}\log\Phi\big(e^{i\theta}\big) &= e^{i\theta}\frac{\Phi'\big(e^{i\theta}\big)}{\Phi\big(e^{i\theta}\big)} \\ &= \frac{1-c^2}{|ce^{i\theta}-1|^2} < 0\end{aligned} \tag{60}$$

since $c = 1/z_\infty > 1$. □

The boundary $b\mathcal{D}_2$ of the second disc $\mathcal{D}_2$ is the image of the inner edge of $\mathcal{A}$.

It is straightforward to show that the inverse of Φ is the Möbius map

$$\Phi^{-1}(\hat{z}) = \frac{z_\infty \hat{z} - 1}{\hat{z} - z_\infty}. \tag{61}$$

4.2 Location of the second disc

Let the radius of the second disc be R, and its centre be at $X \in \mathbb{C}$. Thus

$$|\Phi(z_0) - X|^2 = R^2 \tag{62}$$

at $z_0 \in \{\rho e^{i\theta}; 0 \le \theta < 2\pi\}$, $\rho \equiv e^{-\omega}$. Motivated by the choice $\Im(z_\infty) = 0$ made earlier we will assume that $\Im(X) = 0$. Substituting (55) into (62) and evaluating the result at $z_0 = \rho e^{i\theta}$ we find that

$$(1-cX)^2\rho^2 + 2(X-c)(1-cX)\cos\theta + (X-c)^2 = R^2(c^2\rho^2 - 2c\cos\theta + 1). \tag{63}$$

Since this must be true for all θ we obtain

$$(1-cX)^2\rho^2 + (X-c)^2 = R^2(1+c^2\rho^2), \tag{64}$$

$$(X-c)(1-cX) = -cR^2. \tag{65}$$

Equations (64) and (65) can be solved to yield ρ and c as functions of R and X,

$$c = \frac{1}{2X}\big[(1 + X^2 - R^2) + \sqrt{(1 + X^2 - R^2)^2 - 4X^2}\big], \tag{66}$$

$$\rho = \sqrt{\frac{R^2 - (X - c)^2}{(1 - cX)^2 - c^2R^2}}. \tag{67}$$

5 Construction of flows around two stationary discs

We now have all of the tools that we need to construct general irrotational fluid flows around two stationary discs. The strategy is straightforward : one chooses an F from (53), constructs $W_{\mathcal{C}}$ and then the complex potential $W_{\mathcal{E}} = W_{\mathcal{C}} \circ \log \circ \Phi^{-1}$ on $\mathcal{E}$. The associated fluid velocity is $\widetilde{\Re(dW_{\mathcal{E}})}$.

The only remaining issues concern the values of the constants $\{A_0, A_{r,m}\}$ in (44). The choice for the residue of $\bar{v}$ is easy because the absolute value of circulation is preserved under conformal transformations. Referring back to section 2.5, let $\nu_{\mathcal{U}}$ and $\nu_{\mathcal{V}}$ be the complex velocity 1-forms associated with $W_{\mathcal{U}}$ and $W_{\mathcal{V}}$,

$$\nu_{\mathcal{V}} = dW_{\mathcal{V}}, \tag{68}$$

$$\nu_{\mathcal{U}} = dW_{\mathcal{U}}. \tag{69}$$

Then

$$\varphi^* \nu_{\mathcal{V}} = \nu_{\mathcal{U}} \tag{70}$$

and so

$$\int_{\varphi \circ C} \nu_{\mathcal{V}} = \int_C \nu_{\mathcal{U}} \tag{71}$$

over any closed 1-chain C on $\mathcal{U}$. Therefore, if the orientations of $\varphi \circ C$ and C are the same then each point vortex in $\mathcal{U}$ corresponds to a unique point vortex in $\mathcal{U}$ with the same strength. If the orientations are opposite then the strengths are opposite. Although first order poles in $\bar{v}_{\mathcal{U}}$ on are in one-to-one correspondence to first order poles in $\bar{v}_{\mathcal{V}}$ on $\mathcal{V}$, terms of orders other than -1 do not correspond in general.

5.1 A simple example

Referring back to (53), a trivial example of $W_{\mathcal{C}}$ on the cell $\mathcal{C}$ follows from the choice

$$F(z) = A_0 z \tag{72}$$

and so, from (52),

$$\begin{aligned} W_{\mathcal{C}}(z) &= (A_0 - \bar{A}_0)z \\ &= \frac{\Gamma}{2\pi i} z \end{aligned} \tag{73}$$

where $\Gamma = 2\pi i(A_0 - \bar{A}_0) \in \mathbb{R}$. The corresponding complex potential on the annulus $\mathcal{A}$ is

$$\begin{aligned} W_{\mathcal{A}}(z) &= \log^* W_{\mathcal{C}}(z) \\ &= W_{\mathcal{C}}(\log z) \\ &= \frac{\Gamma}{2\pi i} \log z. \end{aligned} \tag{74}$$

Pulling back $W_{\mathcal{A}}$ to $\mathcal{E}$ with the inverse Möbius map Φ^{-1} yields

$$\begin{aligned} W_{\mathcal{E}}(z) &= \Phi^{-1*} W_{\mathcal{A}}(z) \\ &= W_{\mathcal{A}}\big(\Phi^{-1}(z)\big) \\ &= \frac{\Gamma}{2\pi i} \log\left(\frac{z_\infty z - 1}{z - z_\infty}\right) \\ &= \frac{\Gamma}{2\pi i}[\log(z - 1/z_\infty) - \log(z - z_\infty)] + \dots \end{aligned} \tag{75}$$

where ... indicates an irrelevant constant. The corresponding complex velocity 1-form $\nu_{\mathcal{E}}$ is

$$\begin{aligned}\nu_{\mathcal{E}} &= dW_{\mathcal{E}} \\ &= \frac{\Gamma}{2\pi i}\left[\frac{1}{z-1/z_\infty} - \frac{1}{z-z_\infty}\right]dz.\end{aligned} \tag{76}$$

The flow obtained in $\mathcal{E}$ is the same as that due to two point vortices of opposite strength at $z = z_\infty$ and $z = 1/z_\infty$. We comment that the velocity field $V = \widetilde{\Re(\nu_{\mathcal{E}})}$ satisfies the *Navier-Stokes* [2] equations and the *no-slip* boundary condition at the boundaries of $\{\mathcal{D}_1, \mathcal{D}_2\}$ if both discs are spinning with angular velocities

$$\Omega_1 = -\frac{\Gamma}{2\pi}, \tag{77}$$

$$\Omega_2 = \frac{\Gamma}{2\pi R^2} \tag{78}$$

respectively, where again R is the radius of $\mathcal{D}_2$.

5.2 Vortices and inflows

The sort of F that is most useful to us has the form $F = F_1 + F_2 + F_3$ where

$$F_1(z) = \frac{1}{2}\frac{\Gamma}{2\pi i}z \tag{79}$$

$$F_2(z) = \frac{1}{2}\sum_j \frac{\Gamma_j}{2\pi i}\log\frac{\theta_1\left(\frac{1}{2i}(z-\zeta_j)\mid\frac{i\omega}{\pi}\right)}{\theta_1\left(\frac{1}{2i}(z+\bar{\zeta}_j)\mid\frac{i\omega}{\pi}\right)} \tag{80}$$

$$F_3(z) = 2\bar{U}\sinh\zeta_\infty\frac{d}{dz}\log\theta_1\left(\frac{1}{2i}(z-\zeta_\infty)\,\middle|\,\frac{i\omega}{\pi}\right) \tag{81}$$

where $\zeta_\infty = \log z_\infty$. The motivation behind the judicious choice of the constants in (79), (80) and (81) will become apparent shortly.

The total circulation term F_1 is has already been discussed. F_2 is due to a set of point vortices of strength $\{\Gamma_j\}$ at $\{\zeta_j\}$ in $\mathcal{C}$. The correspondence between the locations $\{\xi_j\}$ of point vortices in $\mathcal{E}$ and $\mathcal{C}$ is $\zeta_j = (\log \circ \Phi^{-1})(\xi_j)$. F_3 becomes the contribution due to an inflow U in $\mathcal{E}$ after pulling back with $\log \circ \Phi^{-1}$. To demonstrate this note that F_3 has the principle part (see (43) and (44))

$$F_{3p}(z) = 2\bar{U} \sinh \zeta_\infty \frac{1}{z - \zeta_\infty}. \tag{82}$$

It follows that near $z = z_\infty$ in $\mathcal{A}$

$$\begin{aligned} (F_3 \circ \log)(z) &= 2\bar{U} \sinh \zeta_\infty \frac{1}{\log(z) - \zeta_\infty} + \dots \\ &= 2\bar{U} \sinh \zeta_\infty \frac{1}{\log(z/z_\infty)} + \dots \\ &= 2\bar{U} \sinh \zeta_\infty \frac{z_\infty}{z - z_\infty} + \dots \end{aligned} \tag{83}$$

where $\dots$ indicates terms that are regular as $z \to z_\infty$. Thus

$$\begin{aligned} (F_3 \circ \log \circ \Phi^{-1})(z) &= 2\bar{U} \sinh \zeta_\infty \frac{z_\infty}{\frac{z_\infty z - 1}{z - z_\infty} - z_\infty} + \dots \\ &= 2\bar{U} \sinh \zeta_\infty \frac{z_\infty (z - z_\infty)}{z_\infty^2 - 1} + \dots \\ &= \bar{U} z + \dots \end{aligned} \tag{84}$$

where $z_\infty = e^{\zeta_\infty}$ has been used and $\dots$ indicates terms that are regular as $|z| \to \infty$ in $\mathcal{E}$. Similarly

$$\begin{aligned} (F_3^\dagger \circ -\log \circ \Phi^{-1})(z) &= 2U \sinh \zeta_\infty \frac{z_\infty}{\frac{z - z_\infty}{z_\infty z - 1} - z_\infty} + \dots \\ &= \bar{U} z_\infty + \dots \end{aligned} \tag{85}$$

and so

$$\begin{aligned} W_{\mathcal{E}}(z) &= (F_3 \circ \log \circ \Phi^{-1})(z) + (F_3^{\dagger} \circ - \log \circ \Phi^{-1})(z) \\ &= \bar{U} z + \dots \end{aligned} \tag{86}$$

leading to the far-field complex velocity 1-form

$$\begin{aligned} \nu_{\mathcal{E}} &= dW_{\mathcal{E}} \\ &= \bar{U} dz + \dots \end{aligned} \tag{87}$$

in $\mathcal{E}$.

6 Representations of θ_1

The choice of representation of θ_1 depends on the application one has in mind. Probably the most computationally efficient representation is [19]

$$\theta_1(z, q) = 2 \sum_{n=0}^{\infty} (-1)^n q^{(n+1)^2} \sin\big[(2n+1)z\big]. \tag{88}$$

The sum in (88) converges very quickly because of the n^2 dependence of the coefficients. An alternative representation, which leads to an expression for a flow field on $\mathcal{A}$ that clearly exhibits its pole structure, is [19]

$$\theta_1(z, q) = 2q^{1/4} \sin z \prod_{n=1}^{\infty} (1 - q^{2n})(1 - q^{2n} e^{2iz})(1 - q^{2n} e^{-2iz}). \tag{89}$$

The former is probably more useful for numerically calculating the complex velocity at a point, whilst the latter is probably more useful if the forces on the discs are to be analytically calculated.

In practice it is often simplest to work on the annulus $\mathcal{A}$ rather than $\mathcal{E}$. This is certainly true when calculating the forces on the discs. Using (88) we note that

$$\begin{aligned}\Psi_1(z) &\equiv \frac{1}{\sqrt{z}}\sum_{n=0}^{\infty}(-1)^n\rho^{n(n+1)}\left(z^{n+1}-z^{-n}\right)\\ &= A_1\theta_1\left(\frac{\log z}{2i}\,\middle|\,\frac{i\omega}{\pi}\right)\end{aligned} \tag{90}$$

where $\rho = e^{-\omega}$ is the inner radius of $\mathcal{A}$ as before and A_1 is constant. From (89) we also have

$$\begin{aligned}\Psi_2(z) &\equiv \left(\sqrt{z}-\frac{1}{\sqrt{z}}\right)\prod_{n=1}^{\infty}\left(z-\rho^{2n}\right)\left(\frac{1}{z}-\rho^{2n}\right)\\ &= A_2\theta_1\left(\frac{\log z}{2i}\,\middle|\,\frac{i\omega}{\pi}\right)\end{aligned} \tag{91}$$

where A_2 is constant. The complex potential $W_{\mathcal{A}}$ on $\mathcal{A}$ stemming from (79) to (81) is

$$W_{\mathcal{A}}(z) = G(z) + G^{\dagger}(1/z) \tag{92}$$

where $G = G_1 + G_2 + G_3$,

$$G_1(z) = \frac{1}{2}\frac{\Gamma}{2\pi i}\log z, \tag{93}$$

$$G_2(z) = \frac{1}{2}\sum_j \frac{\Gamma_j}{2\pi i}\log\frac{\Psi(z/z_j)}{\Psi(\bar{z}_j z)}, \tag{94}$$

$$G_3(z) = \bar{U}(z_\infty - 1/z_\infty)z\frac{d}{dz}\log\Psi(z/z_\infty) \tag{95}$$

and Ψ is either Ψ_1 or Ψ_2.

6.1 The vortex contribution

Examination of (91) reveals that

$$\Psi(1/z) = -\Psi(z) \tag{96}$$

and so, using (94) and (96),

$$\begin{aligned} G_2^\dagger(1/z) &= -\frac{1}{2}\sum_j \frac{\Gamma_j}{2\pi i}\log\frac{\Psi(1/(\bar{z}_j z))}{\Psi(z_j/z)} \\ &= -\frac{1}{2}\sum_j \frac{\Gamma_j}{2\pi i}\log\frac{\Psi(\bar{z}_j z)}{\Psi(z/z_j)} \\ &= G_2(z). \end{aligned} \tag{97}$$

Thus, the contribution to the complex potential from the vortices simplifies to

$$W_{\mathcal{A}2}(z) = \sum_j \frac{\Gamma_j}{2\pi i}\log\frac{\Psi(z/z_j)}{\Psi(\bar{z}_j z)}. \tag{98}$$

If we use representation (90) for Ψ then the associated complex velocity is

$$\bar{v}_{\mathcal{A}2} = v^\dagger_{\mathcal{A}2}(z) = \sum_j \frac{\Gamma_j}{2\pi i}\left(\frac{1}{z_j}\frac{\Xi'(z/z_j)}{\Xi(z/z_j)} - \bar{z}_j\frac{\Xi'(\bar{z}_j z)}{\Xi(\bar{z}_j z)}\right) \tag{99}$$

where

$$\Xi'(z) \equiv \frac{d}{dz}\Xi(z) \tag{100}$$

$$\Xi(z) = \sum_{n=0}^{\infty}(-1)^n \rho^{n(n+1)}\big(z^{n+1} - z^{-n}\big). \tag{101}$$

For example, to lowest order in ρ

$$\Xi(z) = z - 1 + O(\rho) \tag{102}$$

and so

$$v^{\dagger}_{\mathcal{A}2}(z) = \sum_j \frac{\Gamma_j}{2\pi i}\left(\frac{1}{z - z_j} - \frac{1}{z - 1/\bar{z}_j}\right) + O(\rho) \tag{103}$$

which is the complex velocity due to a set of vortices inside the unit circle.

6.2 The inflow contribution

A nice result for the inflow contribution to the complex velocity on $\mathcal{A}$ follows when (91) is used to evaluate (95). It is straightforward to show that

$$\begin{aligned} H(z) &\equiv z\frac{d}{dz}\log\Psi_2(z) \\ &= \frac{1}{2}\frac{z+1}{z-1} + \sum_{n=1}^{\infty}\left(\frac{z}{z-\rho^{2n}} - \frac{1}{1-\rho^{2n}z}\right) \end{aligned} \tag{104}$$

from which follows the remarkably simple expression

$$\begin{aligned} H'(z) &\equiv \frac{d}{dz}H(z) \\ &= -\sum_{n=-\infty}^{\infty}\frac{\rho^{2n}}{(z-\rho^{2n})^2}. \end{aligned} \tag{105}$$

Equation (105) can be used to show that

$$H'(1/z) = z^2 H'(z). \tag{106}$$

Using (95), (104) and (106) the complex velocity $\bar{v}_{\mathcal{A}3}$, where

$$v^{\dagger}_{\mathcal{A}3}(z) = \frac{d}{dz}W_{\mathcal{A}3}(z), \tag{107}$$

$$W_{\mathcal{A}3}(z) = G_3(z) + G^{\dagger}_3(1/z), \tag{108}$$

has the form

$$\bar{v}_{\mathcal{A}3} = v^{\dagger}_{\mathcal{A}3}(z) = \bar{U}(1 - 1/z_\infty^2)H'(z/z_\infty) + U(1 - z_\infty^2)H'(z_\infty z). \tag{109}$$

6.3 The complex velocity on $\mathcal{E}$

Once a complex velocity $\bar{v}_{\mathcal{A}}$ on $\mathcal{A}$ has been established the corresponding complex velocity $\bar{v}_{\mathcal{E}}$ on $\mathcal{E}$ is

$$\bar{v}_{\mathcal{E}} = v^{\dagger}_{\mathcal{E}}(z) = v^{\dagger}_{\mathcal{A}}[\Phi^{-1}(z)]\frac{d\Phi^{-1}}{dz}(z) \tag{110}$$

7 Incorporating relative disc motion

So far, the boundary conditions imposed on the fluid velocity V are suitable for discs $\{\mathcal{D}_1, \mathcal{D}_2\}$ that are fixed with respect to a non-rotating frame of reference. Now let $\mathcal{D}_2$ be translating relative to $\mathcal{D}_1$ with velocity U_2 and let $\{C_1.C_2\}$ be 1-chains with images $\{b\mathcal{D}_1, b\mathcal{D}_2\}$ respectively. The instantaneous no-though-flow conditions at each disc are

$$C_1^* \star \tilde{V} = 0, \tag{111}$$

$$C_2^* \star (\tilde{V} - \tilde{U}_2) = 0. \tag{112}$$

We have discussed how to construct flows that satisfy the no-through-flow condition at each disc and tend to uniformity at spatial infinity. To incorporate a non-trivial boundary condition on $\mathcal{D}_2$ we need an additional contribution to the complex potential discussed above. We will use standard methods to solve Laplace's equation for a stream function subject to the correct boundary conditions.

7.1 Conformal transformations and Laplace's equation

Let $\psi_{\mathcal{E}}$ be a smooth scalar on $\mathcal{E}$ that is a stream function for V i.e.

$$\star_{\mathcal{E}}\tilde{V} = d\psi_{\mathcal{E}}, \tag{113}$$

$$d \star_{\mathcal{E}} d\psi_{\mathcal{E}} = 0, \tag{114}$$

where $\star_{\mathcal{E}}$ is the Hodge map on $\mathcal{E}$ associated with the metric $g_{\mathcal{E}}$. Expressed with respect to a cartesian chart $\{\hat{x}, \hat{y}\}$ on $\mathcal{E}$ the metric $g_{\mathcal{E}}$ has the form

$$g_{\mathcal{E}} = d\hat{x} \otimes d\hat{x} + d\hat{y} \otimes d\hat{y}. \tag{115}$$

Let $g_{\mathcal{A}}$ be the metric on $\mathcal{A}$ and $\{x, y\}$ be a cartesian chart on $\mathcal{A}$,

$$g_{\mathcal{A}} = dx \otimes dx + dy \otimes dy, \tag{116}$$

with origin at the centre of $\mathcal{A}$ and let Φ, as introduced earlier, have the action $\hat{x} + i\hat{y} = \Phi(x + iy)$. For notational simplicity we will not distinguish Φ and the associated map taking $\{x, y\}$ to $\{\hat{x}, \hat{y}\}$ i.e. we write

$$\begin{aligned}(\hat{x}, \hat{y}) &= \Phi(x, y) \\ &\equiv \big(\Re[\Phi(x + iy)], \Im[\Phi(x + iy)]\big)\end{aligned} \tag{117}$$

and so

$$(\Phi^* f)(x, y) = f\big(\Re[\Phi(x + iy)], \Im[\Phi(x + iy)]\big) \tag{118}$$

for any scalar f on $\mathcal{E}$. Let $\star_{\mathcal{A}}$ be the Hodge map associated with $g_{\mathcal{A}}$. That Φ is a conformal map means that locally

$$\Phi^* g_{\mathcal{E}} = \lambda g_{\mathcal{A}} \tag{119}$$

where λ is a scalar on $\mathcal{A}$. Consequences of (119) are

$$\Phi^* \star_{\mathcal{E}} 1 = \lambda \star_{\mathcal{A}} 1, \tag{120}$$

$$\Phi_*^{-1} g_{\mathcal{E}}^{-1} = \frac{1}{\lambda} g_{\mathcal{A}}^{-1}, \tag{121}$$

from which it follows that for any 1-form α on $\mathcal{E}$

$$\Phi^* \star_{\mathcal{E}} \alpha = \star_{\mathcal{A}} \Phi^* \alpha. \tag{122}$$

Pulling back (114) to $\mathcal{A}$ with Φ yields

$$d \star_{\mathcal{A}} d\psi_{\mathcal{A}} = 0, \tag{123}$$

$$\psi_{\mathcal{A}} \equiv \Phi^* \psi_{\mathcal{E}} \tag{124}$$

where $\Phi^* d = d\Phi^*$ and (122) have been used. The boundary conditions (111) and (112) written on $\mathcal{A}$ are

$$C^*_{\mathcal{A}1} d\psi_{\mathcal{A}} = 0, \tag{125}$$

$$C^*_{\mathcal{A}2} d\psi_{\mathcal{A}} = C^*_{\mathcal{A}2} \star_{\mathcal{A}} \Phi^* \tilde{U}_2 \tag{126}$$

where $C_{\mathcal{A}j} \equiv \Phi^{-1} \circ C_{\mathcal{E}j}$ and the images of $\{C_{\mathcal{A}1}, C_{\mathcal{A}2}\}$ and $\{C_{\mathcal{E}1}, C_{\mathcal{E}2}\}$ are the edges of the annulus $\mathcal{A}$ and the boundaries of the discs $\{\mathcal{D}_1, \mathcal{D}_2\}$ respectively. The boundary conditions are satisfied by the choices

$$C^*_{\mathcal{A}1} \psi_{\mathcal{A}} = 0 \tag{127}$$

$$C^*_{\mathcal{A}2} \psi_{\mathcal{A}} = C^*_{\mathcal{A}2} \phi + \kappa \tag{128}$$

where ϕ is a solution of

$$d\phi = \star_{\mathcal{A}} \Phi^* \tilde{U}_2 \tag{129}$$

and κ is an (instantaneous) constant that will be chosen later.

7.2 Solutions to Laplace's equation on $\mathcal{A}$

With respect to the chart $\{\xi, \theta\}$ on $\mathcal{A}$, which is related to $\{x, y\}$ by

$$x + iy = e^{\xi + i\theta}, \tag{130}$$

equation (123) is

$$\frac{\partial^2 \psi}{\partial \xi^2} + \frac{\partial^2 \psi}{\partial \theta^2} = 0 \tag{131}$$

where, for simplicity, the subscript $\mathcal{A}$ has been dropped. That (131) is Laplace's equation written with respect to $\{\xi, \theta\}$ follows from the previous section because the mapping (130) between $\{x, y\}$ and $\{\xi, \theta\}$ can be interpreted as a conformal map from a rectangle in $\mathbb{C}$ to $\mathcal{A}$. Solutions to (131) can be formed out of linear combinations of products of $\{\cosh(n\xi), \sinh(n\xi)\}$ and $\{\cos(n\theta), \sin(n\theta)\}$ where $n \in \mathbb{Z}$, $n \geq 0$. We choose

$$\psi(\xi, \theta) = \sum_{n=1}^{\infty} \frac{\sinh(n\xi)}{\sinh(n\omega)} \big[a_n \cos(n\theta) + b_n \sin(n\theta)\big] \tag{132}$$

because it automatically satisfies the outer edge boundary condition

$$\psi(0, \theta) = 0. \tag{133}$$

Since

$$\tilde{U}_2 = \Re(\bar{u} d\hat{z}), \tag{134}$$

where $\hat{z} = \hat{x} + i\hat{y}$ and $u \equiv d\hat{x}(U_2) + id\hat{y}(U_2)$ is the relative complex velocity of $\mathcal{D}_2$ with respect to $\mathcal{D}_1$, it can be shown that

$$\begin{aligned} \star_{\mathcal{E}} \tilde{U}_2 &= \Im(\bar{u} d\hat{z}) \\ &= d\big[\Im(\bar{u}\hat{z})\big]. \end{aligned} \tag{135}$$

The final expression in (135) follows because u is (instantaneously) constant. If follows from (135) that, using (122), a particular solution to (129) is

$$\phi(z) = \Im\big[\bar{u}\Phi(z)\big] \tag{136}$$

and so the inner edge boundary condition (128) can be written

$$\psi(-\omega, \theta) = \Im\big[\bar{u}\Phi\big(e^{-\omega + i\theta}\big)\big] + \kappa. \tag{137}$$

To match (132) to the boundary condition (137) we insert a Laurent series for $\Phi(z)$ into (137) valid for $|z/z_\infty| < 1$ and equate Fourier components. Using

$$\frac{1}{1 - z} = \sum_{n=0}^{\infty} z^n, \quad |z| < 1 \tag{138}$$

it can be shown that

$$\begin{aligned}\Phi(z) &= \frac{z_\infty z - 1}{z - z_\infty} \\ &= \frac{1}{z_\infty} + \sum_{n=1}^{\infty}\left(\frac{1}{z_\infty^{n+1}} - \frac{1}{z_\infty^{n-1}}\right) z^n, \quad |z/z_\infty| < 1\end{aligned} \tag{139}$$

and we find

$$\begin{aligned}\psi(-\omega,\theta) &= -\sum_{n=1}^{\infty} 2\sinh\zeta_\infty e^{-n(\omega+\zeta_\infty)}\Im\big(\bar{u}e^{in\theta}\big) + \kappa + \dots \\ &= -\sum_{n=1}^{\infty} 2\sinh\zeta_\infty e^{-n(\omega+\zeta_\infty)}\big[\Re(u)\sin(n\theta) - \Im(u)\cos(n\theta)\big] \\ &\quad + \kappa + \dots\end{aligned} \tag{140}$$

where $z_\infty = e^{\zeta_\infty}$ and $\dots$ indicates terms that are independent of θ and can be eliminated by judiciously choosing κ. Evaluating (132) at $\xi = -\omega$ gives

$$\psi(-\omega,\theta) = -\sum_{n=1}^{\infty}\big[a_n\cos(n\theta) + b_n\sin(n\theta)\big] \tag{141}$$

which on comparison with (140) yields

$$a_n = -2\sinh\zeta_\infty\Im(u)e^{-n(\omega+\zeta_\infty)}, \tag{142}$$

$$b_n = 2\sinh\zeta_\infty\Re(u)e^{-n(\omega+\zeta_\infty)} \tag{143}$$

and so

$$\psi(\xi,\theta) = 2\sinh\zeta_\infty\sum_{n=1}^{\infty}\frac{\sinh(n\xi)}{\sinh(n\omega)}e^{-n(\omega+\zeta_\infty)}\Im\big(\bar{u}e^{in\theta}\big). \tag{144}$$

Written in terms of z and z_∞, where $z = e^{\xi+i\theta}$, the above expression has the form

$$\psi(\xi,\theta) = (z_\infty - 1/z_\infty)\sum_{n=1}^{\infty}\left(\frac{\rho}{z_\infty}\right)^n \frac{\rho^n}{1-\rho^{2n}}\Im(\bar{u}z^n + uz^{-n})\Big|_{z=e^{\xi+i\theta}} \quad (145)$$

and so we introduce an additional contribution to the complex potential $W_{\mathcal{A}}$

$$W_{\mathcal{A}4}(z) = (z_\infty - 1/z_\infty)\sum_{n=1}^{\infty}\left(\frac{\rho}{z_\infty}\right)^n \frac{\rho^n}{1-\rho^{2n}}(\bar{u}z^n + uz^{-n}) \quad (146)$$

which, by inspection, is analytic on $\mathcal{A}$. The corresponding complex velocity is

$$\bar{v}_{\mathcal{A}4} = v^{\dagger}_{\mathcal{A}4}(z) = (z_\infty - 1/z_\infty)\sum_{n=1}^{\infty}\left(\frac{\rho}{z_\infty}\right)^n \frac{\rho^n}{1-\rho^{2n}} n(\bar{u}z^{n-1} - uz^{-n-1}). \quad (147)$$

8 Transformation to an inertial frame of reference

So far we have discussed how to construct arbitrary irrotational and incompressible fluid flows around two discs $\{\mathcal{D}_1, \mathcal{D}_2\}$ on $\mathbb{C}$ where $\mathcal{D}_1$ has unit radius and is centred at the origin and $\mathcal{D}_2$ has radius R and is centred on the real axis. The complex velocity $\bar{v}_{\mathcal{E}}$ consists of four contributions due to overall circulation, any number of vortices, an inflow and the relative velocity of the discs,

$$\bar{v}_{\mathcal{E}} = \bar{v}_{\mathcal{E}1} + \bar{v}_{\mathcal{E}2} + \bar{v}_{\mathcal{E}3} + \bar{v}_{\mathcal{E}4}, \quad (148)$$

$$\bar{v}_{\mathcal{E}j} = v^{\dagger}_{\mathcal{A}j}[\Phi^{-1}(z)]\frac{d\Phi^{-1}}{dz}(z), \quad (149)$$

where $\{v^\dagger_{\mathcal{A}2}, v^\dagger_{\mathcal{A}3}, v^\dagger_{\mathcal{A}4}\}$ are given by (99), (109), (147) and

$$\bar{v}_{\mathcal{A}1} = v^\dagger_{\mathcal{A}1}(z) = \frac{\Gamma}{2\pi i}\frac{1}{z}. \tag{150}$$

Our calculation remains valid for an *arbitrary* configuration of two moving rigid discs *at an instant* if we interpret $\bar{v}_{\mathcal{E}}$ as the complex fluid velocity with respect to an appropriately scaled inertial frame of reference that is centred at one of the discs. Let $Z^\sharp_1, Z^\sharp_2 \in \mathbb{C}$ be the instantaneous centres of two circular discs of radii $R_1, R_2 \in \mathbb{R}$ with respect to an arbitrary inertial frame $\mathcal{O}$. Let $u^\sharp_1, u^\sharp_2 \in \mathbb{C}$ be their instantaneous complex velocities with respect to $\mathcal{O}$ and let $z^\sharp = x^\sharp + iy^\sharp \in \mathbb{C}$ be the instantaneous position of any point in the fluid with respect to $\mathcal{O}$. The coordinate $z^\sharp$ is related to the hatted coordinate system $\{\hat{x}, \hat{y}\}$ by

$$\hat{z} = \frac{z^\sharp - Z^\sharp_1}{R_1} e^{-i\phi} \tag{151}$$

where

$$\phi = \mathrm{Arg}(Z^\sharp_2 - Z^\sharp_1) \tag{152}$$

and so the locations $\{z_j\}$ of vortices in $\mathcal{A}$ are related to those with respect to $\mathcal{O}$ by

$$z_j = \Phi^{-1}(\hat{z}_j), \tag{153}$$

$$\hat{z}_j = \frac{z^\sharp_j - Z^\sharp_1}{R_1} e^{-i\phi}. \tag{154}$$

The complex (conjugate) fluid velocity $\bar{v}^\sharp$ with respect to $\mathcal{O}$ is

$$\bar{v}^\sharp = v^{\sharp\dagger}(z^\sharp) = R_1 e^{-i\phi} v^\dagger_{\mathcal{E}}(\hat{z}) + \bar{u}^\sharp_1, \tag{155}$$

the relative disc complex (conjugate) velocity $\bar{u}$ is

$$\bar{u} = \frac{\bar{u}^\sharp_2 - \bar{u}^\sharp_1}{R_1} e^{i\phi} \tag{156}$$

and

$$R = \frac{R_2}{R_1}. \tag{157}$$

The fluid velocity vector field with respect to $\mathcal{O}$ is

$$V^\sharp = \Re(\widetilde{\bar{v}^\sharp dz^\sharp}) \tag{158}$$

where the metric dual is taken with respect to

$$g^\sharp = dx^\sharp \otimes dx^\sharp + dy^\sharp \otimes dy^\sharp. \tag{159}$$

9 Summary

We have presented a method for constructing arbitrary irrotational fluid flows around two arbitrarily translating circular discs of arbitrary location and size. Once $\bar{v}_{\mathcal{E}}$ has been chosen the velocity field $V^\sharp$ can be calculated and (26) used to obtain the Killing drives on the boundaries of the discs. The expression for $\bar{v}_{\mathcal{E}}$ contains the first Jacobi theta function which can be represented in different ways depending on whether or not its pole structure is to be exhibited. If the explicit pole structure of $\bar{v}_{\mathcal{E}}$ is not necessary then a faster converging representation can be used.

Acknowledgements

DAB and RWT are grateful to Orcina Ltd. (Ulverston, UK), TTI and EPSRC for financially supporting this project.

References

[1] Abraham, R., Marsden, J.E., Ratiu, T. *Manifolds, Tensor Analysis and Applications.* Springer-Verlag, (1988).

[2] Batchelor, G.K. *Introduction to Fluid Dynamics.* Cambridge University Press (1967).

[3] Basset, A.B. *A Treatise on Hydrodynamics.* Deighton, Bell & co. (1888).

[4] Blevins, R.D. *Flow Induced Vibration.* Van Nostrand Reinhold, New York (1990).

[5] Bogdan, T.J. *The turbulent twisted magnetic-flux tube gas.* Physics of Fluids **27** (1984), 994–1004.

[6] Burton, D.A., Cao, D., Tucker, R.W., Wang, C.H.T. *On the stability of stay cables under light wind and rain conditions.* Journal of Sound and Vibration (submitted).

[7] Burton, D.A., Hartley, D. & Tucker, R.W. *Vortex-induced fluid forces on accelerating rigid boundaries in 2 dimensions.* Proceedings of the 5th International Seminar on “Geometry, Continua & Microstructure”. Sinaia, Romania, September 26-28 2001, Editura Academiei Romane.

[8] Greenhill, A.G. *Functional Images in Cartesians.* Quarterly Journal of Pure and Applied Mathematics **18** (1882), 356–362.

[9] Huang, L.H. & Yong, J.K. *Hybrid approach to uniform flow past two cylinders.* Journal of Engineering Mechanics **121** (1995), 367–378.

[10] Hicks, W.M. *On the motion of two cylinders in a fluid.* Quarterly Journal of Pure and Applied Mathematics **16** (1879), 113–140 & 193–219.

[11] Lamb, H. *Hydrodynamics* Cambridge University Press (1932) (6th ed.)

[12] Milne-Thomson, L.M. *Theoretical Hydrodynamics.* MacMillan & co. ltd. (London) (1962) (4th ed.)

[13] Morse, P. & Feshbach, H. *Methods of Theoretical Physics.* McGraw-Hill (1953).

[14] Sarpkaya, T. *Vortex-induced oscillations.* Journal of Applied Mechanics **46** (1979), 241–258.

[15] Sarpkaya, T. *Computational methods with vortices : The 1988 Freeman Scholar Lecture.* Journal of Fluids Engineering **111** (1989) 5–52.

[16] Sarpkaya, T. & Schoaff, R.L. *Inviscid model of two-dimensional vortex shedding by a circular cylinder.* AIAA Journal **17** 11 (1979) 1193–1200.

[17] Schlichting, H. *Boundary–Layer Theory,* 6th ed., McGraw–Hill, (1968).

[18] Sun, R. & Chwang, A.T. *Interaction between rotating elliptic cylinder and fixed circular cylinder.* Journal of Engineering Mechanics **125** 7 (1999).

[19] Whittaker, E.T. & Watson, G.N. *A Course of Modern Analysis.* Cambridge University Press (1927) (4th ed.)

[20] Yamamoto, T. *Hydrodynamic forces of multiple circular cylinders.* Journal of the Hydraulics Division, Proceedings of the American Society of Civil Engineers **102** (1976), 1193–1211.

[21] Young, A.D. *Boundary Layers.* BSP Professional Books, (1989).

Hidrodinamičke sile na dva pokretna diska

UDK 514.7, 532.59

U radu se daje detaljna prezentacija jednog prilagodljivog metoda za konstrukciju eksplicitnih izraza za irotaciona i nestišljiva fluidna tečenja oko dva kruta pokretna kružna diska. Takodje se diskutuje kako takvi izrazi mogu da se iskoriste za izračunavanje fluidom izazvanih sila i spregova na diskove pomoću Kilingovih diskova. Zatim se Mebijusovom transformacijom koristeći tehniku konformnog preslikavanja izvodi identifikacija meromorfne funkcije na anularnoj oblasti u $\mathbb{C}$ sa tečenjem oko dva kružna diska. Ovde polovi prvog reda odgovaraju vrtlozima van diskova. Tečenja ka unutrašnjosti se uzimaju u obzir postavljanjem pola drugog reda u anulus koji odgovara beskonačnosti.